State-insensitive bichromatic optical trapping

Bindiya Arora* and M. S. Safronova
Department of Physics and Astronomy, University of Delaware, Newark, Delaware 19716, USA

Charles W. Clark
Joint Quantum Institute, National Institute of Standards and Technology and the University of Maryland, Gaithersburg, Maryland 20899-8410, USA

(Received 7 May 2010; published 19 August 2010)

We study a scheme for state-insensitive trapping of neutral atoms by using light with two independent wavelengths. In particular, we describe the use of trapping and control lasers to minimize the variance of the potential experienced by a trapped Rb atom in ground and excited states. We present calculated values of wavelength pairs for which the $5s$ and $5p_{3/2}$ levels have the same ac Stark shifts in the presence of two laser fields.

DOI: 10.1103/PhysRevA.82.022509 PACS number(s): 32.10.Dk, 37.10.Jk, 31.15.ap, 31.15.ac

I. INTRODUCTION

The emerging advantages of using transitions between different atomic electronic configurations for frequency standards and quantum information processing are accompanied by disadvantages with respect to previous methods in which atomic qubits were hyperfine states of the same configuration. In the latter case, the energy shifts of states induced by external trapping fields are small, and can be calculated to an accuracy that usually does not make a significant contribution to the uncertainty budget. When qubits are associated with different configurations, on the other hand, the magnitude and even the sign of differential field shifts are uncontrolled in the first instance.

The ability to trap neutral atoms inside high-Q cavities in the strong coupling regime is of particular importance for quantum computation and quantum communication schemes, where it is essential to precisely localize and control neutral atoms with minimum decoherence. In a far-detuned optical dipole trap, the potential experienced by an atom in its ground state can be either attractive or repulsive, with respect to the location of peak light intensity, depending on the sign of the ac Stark shift due to the trapping light. Excited-state atoms in the same trap may experience an ac Stark shift with an opposite sign, which affects the fidelity of experiments in which excited states are temporarily occupied, such as the implementation of the Rydberg quantum gate [1–5].

The same problem (i.e., different Stark shifts of two states) affects optical frequency standards based on atoms trapped in optical lattices because it can introduce a significant dependence of the measured frequency of the clock transition upon the lattice wavelength. Katori *et al.* [6] proposed the idea of using a trapping laser tuned to a magic wavelength, λ_{magic}, at which the ac Stark shift of the clock transition is eliminated. The magic wavelength of the $^{87}\text{Sr}\ ^1S_0$-$^3P_0^\circ$ clock transition was found to be 813.5 ± 0.9 nm in Ref. [7] by investigating the wavelength dependence of the carrier linewidth. This magic wavelength was later determined with even higher precision to be 813.427 35(40) nm [8]. In a cavity quantum electrodynamics experiment, McKeever *et al.* [9] demonstrated state-insensitive trapping of Cs atoms at $\lambda_{\text{magic}} \approx 935$ nm while still maintaining a strong coupling for the $6p_{3/2}$-$6s_{1/2}$ transition.

Magic wavelengths for the np-ns transitions in alkali-metal atoms from Na to Cs have been previously calculated by Arora *et al.* [10], using a relativistic all-order method. This was accomplished by matching the ac polarizabilities of the atomic np_j and ns states. The data in Ref. [10] provide a wide range of magic wavelengths for alkali-metal atoms. In the case of the $np_{3/2}$-ns transitions, the magic wavelengths need to be determined separately for the $m_j = \pm 1/2$ and $m_j = \pm 3/2$ states, due to the rank-2 tensor contribution to the polarizability of the $np_{3/2}$ level. Furthermore, there is a substantial reduction in the number of magic wavelengths for the $m_j = \pm 3/2$ states due to selection rules for linear polarization. For instance, three out of the six values of λ_{magic} suggested for the $5p_{3/2}$-$5s$ transition in Rb are present only for the $m_j = \pm 1/2$ states. In such cases, the magic wavelength becomes dependent on the particular hyperfine state of the atom. Some of the magic wavelengths are also in regions that are inconvenient for present laser technology. Out of the remaining three wavelengths considered in [10], the λ_{magic} at 791 nm has opposite signs for the Stark shifts for $m_j = \pm 3/2$ and $m_j = \pm 1/2$ states, which makes this wavelength of limited practical use. The second magic wavelength at 776 nm is in close proximity to the Rb $5p$-$5d$ resonance transition at 775.8 nm, which could mediate undesired two-photon transitions. The third magic wavelength at 637 nm exists for all states, but its corresponding polarizability is too small for convenient trapping (it is $-500\, a_0^3$, where a_0 is the Bohr radius). In summary, the single-laser scheme offers few cases in which the magic wavelengths are convenient for state-insensitive trapping of Rb atoms [10].

In this paper, we investigate an obvious mechanism for remediating uncontrolled frequency shifts in transitions between different configurations: the application of a second, "control," optical field to a system of optically trapped atoms. We outline the general principles of this approach, and apply it in detail to some cases in Rb. Rubidium is chosen because it offers a baseline of comparison with previous, monochromatic attempts at control, and this serves to illustrate the advantages

*Permanent address: Department of Physics, Guru Nanak Dev University, Amritsar 143005, Punjab, India.

of the bichromatic approach that we believe will have wide applicability.

Specifically, we find the combinations of two wavelengths that allow us to match ac Stark shifts of the Rb atom in $5s$ and $5p_{3/2}$ states. In this scheme, a combination of trapping and control lasers allows one to minimize the difference in the trapping potentials experienced by the atom in the ground and excited states. This approach significantly increases the number of wavelengths at which state-insensitive trapping experiments can be conducted.

We note that this scheme involves maintaining a fixed intensity ratio of two lasers to a certain precision over the extent of the experimentally relevant region. We have investigated the sensitivity of the bichromatic scheme to variation in the intensity ratio. The results are described at the end of Sec. III. The specific geometric configuration that will maximize the ac Stark shift cancellation over the required region will depend upon a number of experimental parameters, such as laser wavelengths, polarization, stabilization of lasers, and trap configuration. We note that there has been an experimental demonstration of light-shift engineering using an auxiliary laser to implement spatially selective optical lattice loading by Griffin *et al.* [11].

The first step in the realization of this scheme is to calculate the Stark shifts of the $5s$ and $5p_{3/2}$ states of the Rb atom as a function of frequency. We use the relativistic all-order method [10,12,13] for the calculation of the reduced electric-dipole matrix elements involved in the evaluation of frequency-dependent polarizabilities. In the second step, we calculate the shift in energies of atomic states as a function of the two laser frequencies. The wavelengths are determined where the ac Stark shifts of the $5s$ and $5p_{3/2}$ levels match according to criteria that are described in the following. Several specific cases are illustrated in detail.

II. FREQUENCY-DEPENDENT POLARIZABILITY

The second-order energy shift ΔE of a monovalent atom in a state v is parameterized as the sum of scalar $\alpha_0(\omega)$ and tensor $\alpha_2(\omega)$ polarizabilities

$$\Delta E = -\frac{1}{2}\alpha_0(\omega)\epsilon^2 - \frac{1}{2}\alpha_2(\omega)\frac{3m_j^2 - j_v(j_v+1)}{j_v(2j_v-1)}\epsilon^2, \qquad (1)$$

where the laser frequency ω is assumed to be several linewidths off-resonance, j_v is the angular momentum, ϵ is the rms magnitude of the electric field, and the polarization vector of the linearly polarized light defines the z direction. The valence contribution to frequency-dependent scalar and tensor polarizability is evaluated as the sum over intermediate k states allowed by the electric-dipole transition rules [14]

$$\begin{aligned}\alpha_0^v(\omega) &= \frac{2}{3(2j_v+1)}\sum_k \frac{\langle k\|d\|v\rangle^2(E_k-E_v)}{(E_k-E_v)^2-\omega^2},\\ \alpha_2^v(\omega) &= -4C\sum_k(-1)^{j_v+j_k+1}\begin{Bmatrix} j_v & 1 & j_k\\ 1 & j_v & 2\end{Bmatrix}\\ &\quad\times\frac{\langle k\|d\|v\rangle^2(E_k-E_v)}{(E_k-E_v)^2-\omega^2},\end{aligned} \qquad (2)$$

where C is given by

$$C = \left[\frac{5j_v(2j_v-1)}{6(j_v+1)(2j_v+1)(2j_v+3)}\right]^{1/2} \qquad (3)$$

and $\langle k\|d\|v\rangle$ are the reduced electric-dipole matrix elements. The experimental energies E_i of the dominant states contributing to this sum have been compiled for the alkali atoms in Refs. [15,16]. In addition to the scalar and tensor valence contributions, there is a scalar core contribution to the polarizability, $\alpha_{\rm core}$. For the frequency range considered in this work, $\alpha_{\rm core}$ has a very small ω dependence. The static core polarizability value calculated using a random-phase approximation [17] has been used in our calculations without loss of accuracy (i.e., uncertainty of this term gives negligible contribution to the total uncertainty).

Unless stated otherwise, we use atomic units [a.u.] for all matrix elements and polarizabilities throughout this paper: the numerical values of the elementary charge e, the reduced Planck constant $\hbar = h/2\pi$, and the electron mass m_e, are set equal to 1. The atomic unit for polarizability can be converted to SI units via α/h [Hz/(V/m)^2] $= 2.488\,32 \times 10^{-8}\alpha$ [a.u.], where the conversion coefficient is $4\pi\epsilon_0 a_0^3/h$ and the Planck constant h is factored out to provide direct conversion into frequency units; a_0 is the Bohr radius and ϵ_0 is the electric constant.

The ground and excited state ac polarizabilities of the alkali-metal atoms were previously calculated accurately in Refs. [10,13,18,19]. A detailed description of the polarizability calculations for atomic Rb is given in Refs. [10,13]. Briefly, the sums over intermediate states k in the formulas are separated into a dominant part $\alpha_{\rm main}$ that contains the first few terms and a remainder $\alpha_{\rm tail}$. In our Rb calculations, we include all ns states up to $10s$ and all nd states up to $9d$ in the $\alpha_{\rm main}$ term. The $\alpha_{\rm tail}$ contribution is calculated in the Dirac-Fock (DF) approximation. We use a complete set of DF wave functions on a nonlinear grid generated using B-splines [20] constrained to a spherical cavity. A cavity radius of 220 a_0 is chosen to accommodate all valence orbitals of $\alpha_{\rm main}$. The basis set consists of 70 splines of order 11 for each value of the relativistic angular quantum number κ.

In the calculation of the main term, the $5p_{3/2}$-$5s$ matrix elements are taken from Ref. [21], and the $5p_{3/2}$-$4d_j$ $E1$ matrix elements are taken to be the recommended values derived in Ref. [22] from the Stark shift measurements reported in [23]. We use the all-order method (linearized version of the coupled cluster approach), which sums infinite sets of many-body perturbation theory terms, for the calculation of all other matrix elements in the dominant part $\alpha_{\rm main}$. A detailed description of the all-order method is given in Refs. [12,24]. For some matrix elements, it was possible to carry out semi-empirical scaling of the all-order values to include some additional important higher-order corrections. The scaling procedure has been described in Refs. [12,14,25]. The resulting frequency-dependent polarizabilities are used to find convenient combinations of trap and control laser wavelengths that yield the same ac Stark shift for Rb atoms in the ground and excited $5p_{3/2}$ levels.

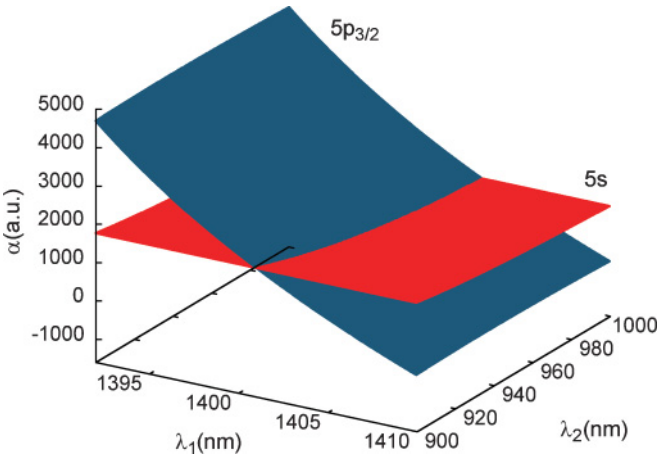

FIG. 1. (Color online) Surface plot for the $5s$ and $5p_{3/2}$ $m_j = \pm 1/2$ state polarizabilities as a function of laser wavelengths λ_1 and λ_2 for equal intensities of both lasers.

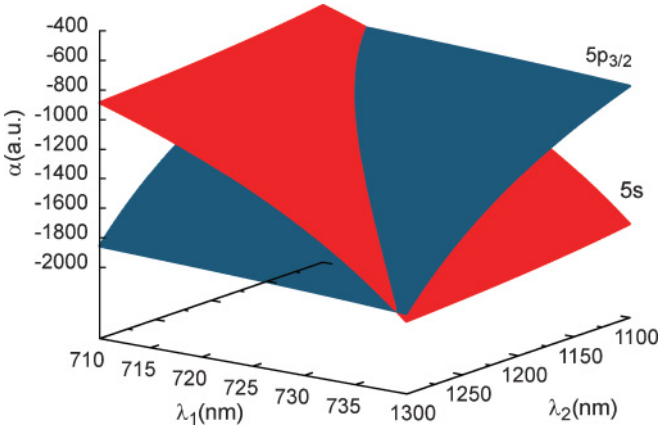

FIG. 2. (Color online) Surface plot for the $5s$ and $5p_{3/2}$ $m_j = \pm 3/2$ state polarizabilities as a function of laser wavelengths λ_1 and λ_2 for equal intensities of both lasers.

III. RESULTS

In this section, we list a few appropriate combinations found for control and trap laser wavelengths where the $5s$ and $5p_{3/2}$ state polarizabilities of Rb are closely matched. For monochromatic light, a magic wavelength is represented by the point at which two curves, $\alpha_{5s}(\omega)$ and $\alpha_{5p}(\omega)$, intersect as a function of the frequency ω. In the bichromatic case, on the other hand, we have two additional degrees of freedom, the control frequency and the ratio of laser intensities. Thus, bichromatic magic wavelengths are represented as curves resulting from the intersection of surfaces.

To illustrate this point, we display sample cases of such surface plots for the $m_j = \pm 1/2$ and $m_j = \pm 3/2$ states in Figs. 1 and 2, respectively. The intensity of both lasers is taken to be the same, so that the energy-level shift is proportional to the sum of two polarizabilities. This is plotted on the z axis. The trap and control laser wavelengths are given on the x and y axes, respectively. The total polarizability of the $5p_{3/2}$ state depends upon its m_j quantum number, and it is calculated as a sum or difference of the scalar α_0 and tensor α_2 polarizabilities [i.e., $\alpha(5p_{3/2}) = \alpha_0 - \alpha_2$ for $m_j = \pm 1/2$ states and $\alpha(5p_{3/2}) = \alpha_0 + \alpha_2$ for $m_j = \pm 3/2$ states]. Therefore, we discuss the results for $m_j = \pm 1/2$ and $m_j = \pm 3/2$ states separately. We also find some appropriate trap and control laser wavelength combinations that have similar magic wavelengths for each m_j state. As illustrated by Figs. 1 and 2, there is a large number of possible combinations of trap and control wavelengths that will result in the same ac Stark shift of both levels.

In Table I, we list a number of sample trap and control wavelength combinations which can be used for state-insensitive trapping of Rb atoms in the $5s$ and $5p_{3/2}$ states. Out of a number of combinations found, we list only those where one of the laser wavelengths is twice the other. This is a case of particular practical interest since it is attainable by frequency doubling of the longer-wavelength laser. The combinations are listed for various trap and control laser intensity ratios as indicated to illustrate the ability to tune the magic wavelength pairs by varying the relative intensities.

The percentage difference between the total polarizabilities of the $5s$ and $5p_{3/2}$ states for the cases listed in Table I is less than 1% taking into account uncertainties

We discuss the magic wavelengths for the $m_j = \pm 1/2$ states first. For equal intensities, the combination with $\lambda_1 =$ 788 nm and $\lambda_2 = 1576$ nm, may be particularly useful since the resulting polarizability is positive and the atoms in red detuned traps are attracted toward the maximum of the field intensity [26,27]. Applying a control laser with double the trap laser wavelength creates a deeper trapping potential for the atom in the ground state and minimizes the difference between the Stark shifts for the ground and excited states. For the $5p_{3/2}, m_j = 1/2$ state the polarizability is negative at 788 nm ($-10\,279\,a_0^3$) and larger and positive at 1576 nm ($15\,194\,a_0^3$). The uncertainties in the polarizabilities at combinations which are close to resonance wavelengths are generally higher. The value of $\alpha^{\rm sum}$ for some of the combinations in Table I is negative, so that the atoms become low-field seekers. A number of groups have suggested blue detuned or dark optical traps where atoms are surrounded by repulsive light fields and therefore are captured in dark regions without light [26,28]. In contrast to the monochromatic case, where very few convenient magic wavelengths were found for $m_j = \pm 3/2$ states, a number of "dark" magic wavelengths for Rb are found in the present bichromatic treatment.

We also found a few laser wavelength combinations that support state-insensitive simultaneous trapping for all m_j states. Examples of such cases are grouped together in the first few rows of Table I. The magic wavelength combination for the $|m_j| = 1/2$ case is given first, and the corresponding $|m_j| = 3/2$ magic wavelength combination is given in the following row. We illustrate the example of such magic wavelength combinations (listed in rows 3 and 4 of Table I) in Fig. 3, where we plot surfaces of the $5s$ and $5p_{3/2}$ $|m_j| = 1/2, 3/2$ state polarizabilities for $\lambda_1 = 806$–826 nm and $\lambda_2 = 1615$–1645 nm. The intensities of both lasers are taken to be equal.

As we mentioned in the Introduction, our scheme involves maintaining a fixed intensity ratio of two lasers to a certain precision. We study the effect of variation in the intensity ratio $(\epsilon_2/\epsilon_1)^2$ on the polarizabilities of the $5s$ and $5p_{3/2}m_j$ states at magic combinations of the trap and control wavelengths by

TABLE I. Magic combinations of the trap and control wavelengths λ_1, $\lambda_2 = 2\lambda_1$ for the $5p_{3/2}m_j$-$5s$ transition in Rb and the corresponding sum of polarizabilities at these wavelengths. The wavelengths (in vacuum) are given in nm and polarizabilities are given in atomic units. ϵ_1^2 and ϵ_2^2 represent the intensities of the two laser beams, respectively. $\alpha^{\rm sum} = \alpha_1 + (\epsilon_2/\epsilon_1)^2\alpha_2$, so that the energy level shift is proportional to $\alpha^{\rm sum}\epsilon_1^2$.

$(\epsilon_2/\epsilon_1)^2$	$\lvert m_j\rvert$	λ_1	λ_2	$\alpha^{\rm sum}(5s)$	$\alpha^{\rm sum}(5p_{3/2})$
1	1/2	788	1576	4990(18)	4914(190)
1	3/2	785	1570	13 240(26)	13 332(210)
1	1/2	814	1628	5189(5)	5194(94)
1	3/2	810	1620	6086(6)	6070(100)
2	1/2	784.3	1568.6	16 819(30)	16 069(436)
2	3/2	782.7	1565.4	30 086(50)	29 715(470)
2	1/2	798.5	1597	17 189(18)	17 297(260)
2	3/2	799	1598	15 611(16)	15 874(260)
3	1/2	782.9	1565.8	28 017(46)	27 317(700)
3	3/2	781.9	1563.8	46 328(70)	46 387(740)
3	1/2	796.8	1593.6	29 026(34)	29 336(410)
3	3/2	797.2	1594.4	24 820(28)	25 059(402)
1	1/2	715	1430	−1047(2)	−1031(84)
1	1/2	974–978	1948–1956	1271(1)–1257(1)	1279–1240(34)
1/2	1/2	727	1454	−1641(2)	−1648(55)
1/2	3/2	787.4	1574.8	6109(20)	6054(100)
1/3	1/2	736	1472	−2113(3)	−2094(50)
1/3	1/2	748	1496	−2963(4)	−2988(80)
1/3	3/2	576	1152	−152(1)	−153(34)
1/3	3/2	639	1278	−425(1)	−422(44)

varying the intensity ratio by 1% to 20% for the examples from Table I. The results are summarized in Table II. The last column gives the difference between $\alpha^{\rm sum}(5s)$ and $\alpha^{\rm sum}(5p_{3/2})$ relative to $\alpha^{\rm sum}(5s)$ in percent.

Our studies indicate that small (around 1%) fluctuation in the intensity ratio does not significantly affect the degree of Stark shift cancellation. Larger variations in the intensity ratios (5%–20%) cause increased differences in Stark shifts of two levels, but would still yield a large degree of cancellation.

The magic wavelength may be further tuned by adjusting the intensity ratio of the two lasers as illustrated in Fig. 4.

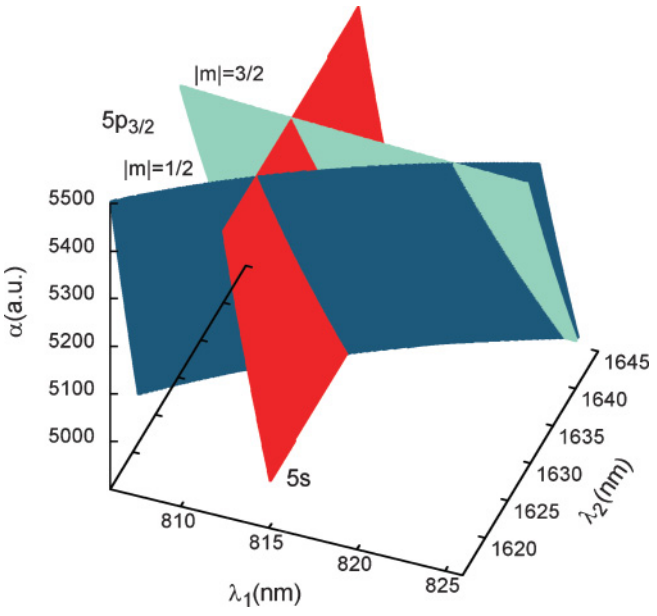

FIG. 3. (Color online) Magic wavelength pairs for $\lambda_1 =$ 806–826 nm and $\lambda_2 =$ 1615–1645 nm and equal intensities of both lasers.

TABLE II. Effect of variation in the intensity ratio $(\epsilon_2/\epsilon_1)^2$ on the polarizabilities of the $5s$ and $5p_{3/2}m_j$ states at magic combinations of the trap and control wavelengths. The wavelengths (in vacuum) are given in nm and polarizabilities are given in atomic units. ϵ_1^2 and ϵ_2^2 represent the intensities of the two laser beams, respectively. $\alpha^{\rm sum} = \alpha_1 + (\epsilon_2/\epsilon_1)^2\alpha_2$, so that the energy-level shift is proportional to $\alpha^{\rm sum}\epsilon_1^2$. Last column gives relative difference between $\alpha^{\rm sum}(5s)$ and $\alpha^{\rm sum}(5p_{3/2})$.

$\lvert m_j\rvert$	λ_1	λ_2	$(\epsilon_2/\epsilon_1)^2$	$\alpha^{\rm sum}(5s)$	$\alpha^{\rm sum}(5p_{3/2})$	Dif.
1/2	788	1576	1	4990(18)	4914(190)	1.5%
			0.99	4986(18)	4763(190)	4.5%
			1.01	4994(18)	5066(190)	1.4%
			1.05	5011(18)	5674(200)	13%
3/2	785	1570	1	13 240(26)	13 332(210)	0.7%
			1.01	13 245(26)	13 462(220)	1.6%
			1.10	13 282(26)	14 635(240)	10%
			1.20	13 325(26)	15 938(250)	20%
1/2	814	1628	1	5189(5)	5194(94)	0.1%
			1.01	5193(5)	5273(95)	1.5%
			1.10	5230(5)	5989(100)	14.5%
1/2	974	1948	1	1271(1)	1279(34)	0.6%
			1.05	1290(1)	1412(35)	9.5%

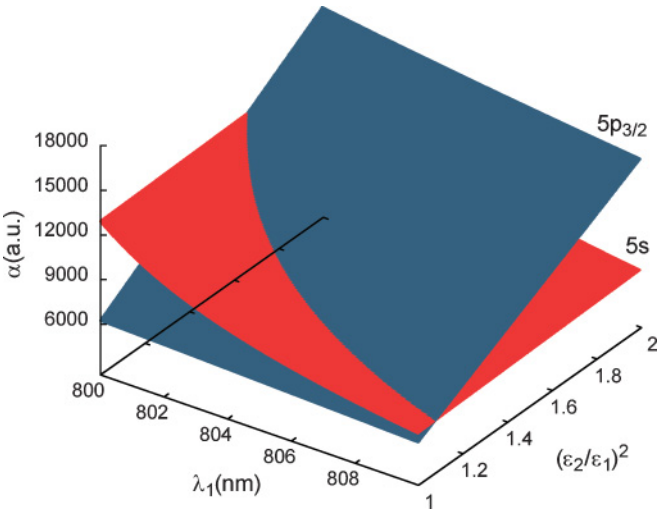

FIG. 4. (Color online) Magic wavelength for the $5s$ and $5p_{3/2}$ $m_j = \pm 1/2$ states for $\lambda_1 = 800$–810 nm and $\lambda_2 = 2\lambda_1$ for various intensities of both lasers. The intensity ratio $(\epsilon_2/\epsilon_1)^2$ ranges from 1 to 2.

The magic wavelength for the $5s$ and $5p_{3/2}$ $|m_j| = 1/2$ states for $\lambda_1 = 800$–810 nm and $\lambda_2 = 2\lambda_1$ are shown for various intensities of both lasers. The intensity ratio $(\epsilon_2/\epsilon_1)^2$ ranges from 1 to 2. This figure also illustrates the variation of ac Stark shift cancellation with the large (by a factor of 2) change in the intensity ratio.

IV. CONCLUSION

In summary, we have explored a bichromatic scheme for state-insensitive optical trapping of the Rb atom. Due to the extensive development of first-principles atomic structure theory, semiempirical corrections, and computational methodology we are able to explore a wide range of parameter space with reasonable confidence in the uncertainties of our calculations. We have recently completed a comprehensive survey of calculations of dc polarizabilities for which there exist copious experimental data for comparison within the clearly stated ranges of uncertainty [29]. In this paper, we specifically explored a case of the Rb atom, where the magic wavelengths associated with monochromatic trapping were sparse and relatively inconvenient. We have found that the bichromatic approach yields a number of promising wavelength pairs which are discovered with straightforward parameter choices such as equal laser intensities and $\lambda_2 = 2\lambda_1$. The methodology developed in this work allows us to explore specific cases of interest that may arise in the future experiments where it is essential to precisely localize and control neutral atoms with minimum decoherence.

ACKNOWLEDGMENTS

This research was performed under the sponsorship of the U.S. Department of Commerce, National Institute of Standards and Technology, and was supported by the National Science Foundation under Physics Frontiers Center Grant No. PHY-0822671.

[1] E. Urban *et al.*, Nature Phys. **5**, 110 (2009).
[2] A. Gaëtan *et al.*, Nature Phys. **5**, 115 (2009).
[3] D. Jaksch, J. I. Cirac, P. Zoller, S. L. Rolston, R. Cote, and M. D. Lukin, Phys. Rev. Lett. **85**, 2208 (2000).
[4] M. D. Lukin, M. Fleischhauer, R. Cote, L. M. Duan, D. Jaksch, J. I. Cirac, and P. Zoller, Phys. Rev. Lett. **87**, 037901 (2001).
[5] M. S. Safronova, C. J. Williams, and C. W. Clark, Phys. Rev. A **67**, 040303 (2003).
[6] H. Katori, T. Ido, and M. Kuwata-Gonokami, J. Phys. Soc. Jpn. **68**, 2479 (1999).
[7] M. Takamoto and H. Katori, Phys. Rev. Lett. **91**, 223001 (2003).
[8] A. D. Ludlow *et al.*, Science **319**, 1805 (2008).
[9] J. McKeever, J. R. Buck, A. D. Boozer, A. Kuzmich, H.-C. Nägerl, D. M. Stamper-Kurn, and H. J. Kimble, Phys. Rev. Lett. **90**, 133602 (2003).
[10] B. Arora, M. S. Safronova, and C. W. Clark, Phys. Rev. A **76**, 052509 (2007).
[11] P. F. Griffin, K. J. Weatherill, S. G. MacLeod, R. M. Potvliege, and C. S. Adams, New J. Phys. **8**, 11 (2006).
[12] M. S. Safronova, W. R. Johnson, and A. Derevianko, Phys. Rev. A **60**, 4476 (1999).
[13] M. S. Safronova, B. Arora, and C. W. Clark, Phys. Rev. A **73**, 022505 (2006).
[14] M. S. Safronova and C. W. Clark, Phys. Rev. A **69**, 040501(R) (2004).
[15] C. E. Moore, *Atomic Energy Levels*, Vol. 35 of *Natl. Bur. Stand. Ref. Data Ser.* (U.S. Government Printing Office, Washington DC, 1971).
[16] J. Sansonetti, W. Martin, and S. Young, *Handbook of Basic Atomic Spectroscopic Data*, version 1.1.2 (National Institute of Standards and Technology, Gaithersburg, MD, 2007).
[17] W. R. Johnson, D. Kolb, and K.-N. Huang, At. Data Nucl. Data Tables **28**, 334 (1983).
[18] A. Derevianko, W. R. Johnson, M. S. Safronova, and J. F. Babb, Phys. Rev. Lett. **82**, 3589 (1999).
[19] C. Zhu, A. Dalgarno, S. G. Porsev, and A. Derevianko, Phys. Rev. A **70**, 032722 (2004).
[20] M. S. Safronova, C. J. Williams, and C. W. Clark, Phys. Rev. A **69**, 022509 (2004).
[21] U. Volz and H. Schmoranzer, Phys. Scr., T **65**, 48 (1996).
[22] B. Arora, M. S. Safronova, and C. W. Clark, Phys. Rev. A **76**, 052516 (2007).
[23] K. E. Miller, D. Krause, and L. R. Hunter, Phys. Rev. A **49**, 5128 (1994).
[24] S. A. Blundell, W. R. Johnson, Z. W. Liu, and J. Sapirstein, Phys. Rev. A **40**, 2233 (1989).
[25] S. A. Blundell, W. R. Johnson, and J. Sapirstein, Phys. Rev. A **43**, 3407 (1991).
[26] T. Puppe, I. Schuster, A. Grothe, A. Kubanek, K. Murr, P. W. H. Pinkse, and G. Rempe, Phys. Rev. Lett. **99**, 013002 (2007).
[27] M. Weber, Ph.D. thesis, University of Munich, 2005.
[28] H. Stecher, H. Ritsch, P. Zoller, F. Sander, T. Esslinger, and T. W. Hansch, Phys. Rev. A **55**, 545 (1997).
[29] J. Mitroy, M. S. Safronova, and C. W. Clark (2010), e-print arXiv:1004.3567.